

mView™ REPORT

Effect of ERR Agonist in Mouse Heart Post Pressure Overload

WASH-02-20VW+

CLIENT: Washington University School of Medicine
Cyrielle Billon, PhD

AUTHOR: James Sollome, PhD
APPROVAL: Brian Ingram, PhD
DATE: January 29, 2021



Table of Contents

Objective	3
Experimental Procedures	3
Results and Biological Interpretation	3
Metabolite Summary and Significantly Altered Biochemicals	3
Biological Interpretation	7
Conclusions	17
Study Parameters	18
Data Quality: Instrument and Process Variability	18
Appendix	19
Metabolon Platform	19
Statistical Methods and Terminology.....	23

Objective

Purpose of Experiment

The goal of this study was to evaluate the metabolic effect of ERR agonists in mouse heart post pressure overload and in skeletal muscle.

Experimental Procedures

Experimental design

Metabolon received 32 mouse heart tissue and 14 mouse quadricep tissue samples on November 11, 2021. Global metabolic profiles were determined from the experimental groups outlined in the table below.

Group Name	Cohort	Description	n	
			Heart	Muscle
Vehicle Sham	1	Heart tissue vehicle, sham surgery	4	
Vehicle TAC	1	Heart tissue vehicle, TAC surgery	8	
SLU915 Sham	1	Heart tissue SLU915, sham surgery	4	
SLU915 TAC	1	Heart tissue SLU915, TAC surgery	6*	
WT	3	Heart tissue WT	5	
klf15	3	Heart tissue klf19	5	
Vehicle	2	Mouse quadricep Vehicle		7
SLU-PP-332	2	Mouse quadricep SLU-PP-332		7

* Note that 1 sample (Client ID: FB06212574) belonging to the SLU915 TAC group was excluded from the analysis due to it having a low response during data collection.

Results and Biological Interpretation

Metabolite Summary and Significantly Altered Biochemicals

The present heart dataset comprises a total of 855 biochemicals, 787 compounds of known identity (named biochemicals) and 68 compounds of unknown structural identity (unnamed biochemicals). The muscle dataset comprises a total of 711 biochemicals, 663 compounds of known identity (named biochemicals) and 48 compounds of unknown structural identity (unnamed biochemicals). Following normalization to mass of sample extracted for heart tissue (equal mass was extracted for muscle tissue samples, so no additional normalization was performed on muscle samples prior to statistical analysis),

log transformation and imputation of missing values, if any, with the minimum observed value for each compound, 2-way ANOVA or Welch's two-sample *t*-test analyses were used to identify biochemicals that differed significantly between experimental groups. A summary of the numbers of biochemicals that achieved statistical significance ($p \leq 0.05$), as well as those approaching significance ($0.05 < p < 0.10$), is shown below.

An estimate of the false discovery rate (*q*-value) is calculated to take into account the multiple comparisons that normally occur in metabolomic-based studies. For example, when analyzing 200 compounds, we would expect to see about 10 compounds meeting the $p \leq 0.05$ cut-off by random chance. The *q*-value describes the false discovery rate; a low *q*-value ($q < 0.10$) is an indication of high confidence in a result. While a higher *q*-value indicates diminished confidence, it does not necessarily rule out the significance of a result. Other lines of evidence may be taken into consideration when determining whether a result merits further scrutiny. Such evidence may include a) significance in another dimension of the study, b) inclusion in a common pathway with a highly significant compound, or c) residing in a similar functional biochemical family with other significant compounds. Refer to the Appendix for general definitions and further descriptions of false discovery rate and other statistical tests used at Metabolon.

Muscle:

Statistical Comparisons - Mouse Quadricep Tissue	
Welch's Two-Sample <i>t</i> -Test	<u>SLU-PP-332</u> VEHICLE
Total biochemicals $p \leq 0.05$	98
Biochemicals (↑↓)	96 2
Total biochemicals $0.05 < p < 0.10$	46
Biochemicals (↑↓)	40 6

Heart:

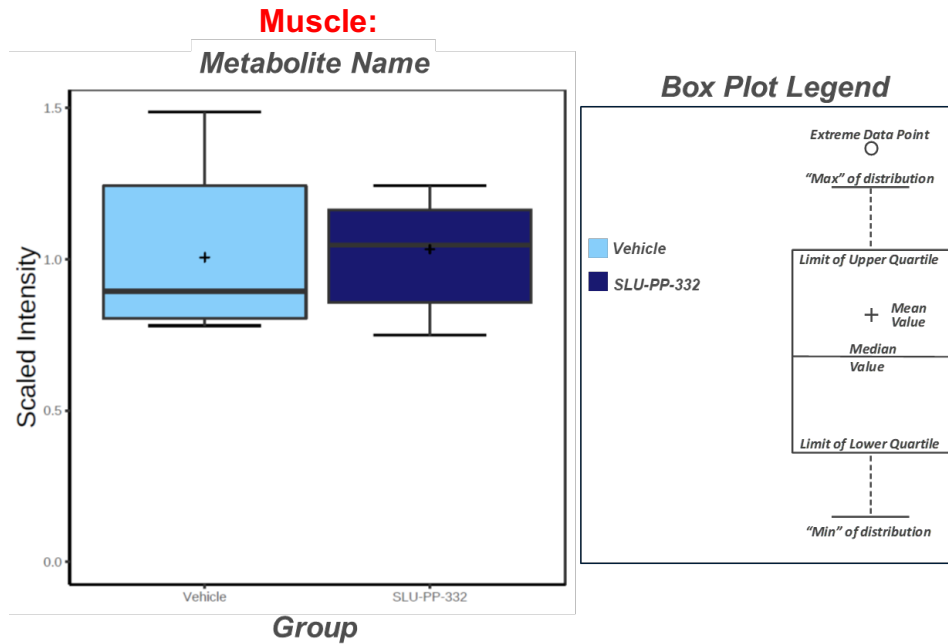
Statistical Comparisons - Mouse Heart Tissue	
Welch's Two-Sample <i>t</i> -Test	<u>KLF15 MASS</u> WT MASS
Total biochemicals $p \leq 0.05$	10
Biochemicals (↑↓)	6 4
Total biochemicals $0.05 < p < 0.10$	21
Biochemicals (↑↓)	14 7

Heart:

Statistical Comparisons - Mouse Heart Tissue				
ANOVA Contrasts	SHAM SLU915 MASS SHAM VEHICLE MASS	TAC SLU915 MASS SHAM SLU915 MASS	TAC SLU915 MASS TAC VEHICLE MASS	TAC VEHICLE MASS SHAM VEHICLE MASS
Total biochemicals $p \leq 0.05$	241	38	166	261
Biochemicals (↑↓)	46 195	23 15	77 89	76 185
Total biochemicals $0.05 < p < 0.10$	59	47	61	74
Biochemicals (↑↓)	23 36	28 19	33 28	22 52

Statistical Comparisons - Mouse Heart Tissue			
Two-Way ANOVA	SURGERY MAIN EFFECT MASS	TREATMENT MAIN EFFECT MASS	SURGERY:TREATMENT INTERACTION MASS
Total biochemicals $p \leq 0.05$	184	248	117
Total biochemicals $0.05 < p < 0.10$	65	67	71

We have also included in the electronic deliverables, a file with data for each biochemical displayed as box plots like that shown in the example figure below.



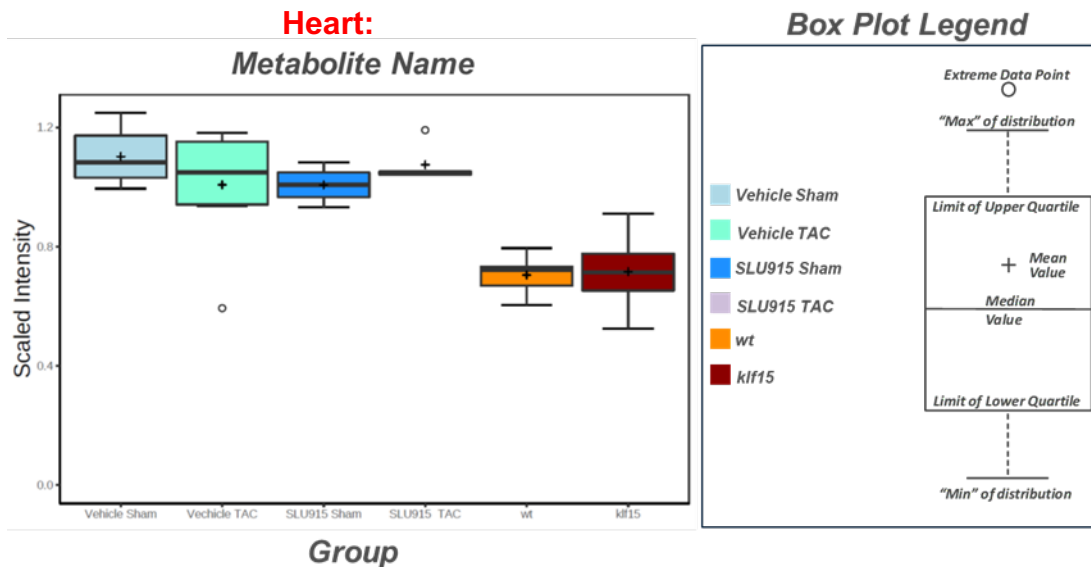


Figure 1. Visualization of the study data in box plot format and the legend for box plots used in this report (heart or muscle samples). Box plots are used to convey the spread of the data with the middle 50% of the data represented by the shaded boxes and the whiskers reporting the range of the data. The solid bar across the box represents the median value of those measured while the + is the mean. Data are scaled such that the median value measured across all samples was set to 1.0. Any outliers are shown as dots outside the whiskers of the plot.

Biological Interpretation

Estrogen Related Receptors (ERRs) are a subgroup of nuclear receptors involved in the regulation of cellular metabolism, energy homeostasis, and in the etiology of metabolic skeletal muscle disorders ([PMID: 32683181](#) [32897058](#)). Hypertension can result in maladaptive cardiomyocyte hypertrophy, which can further lead to ischemic injury (myocardial infarction) and/or reduced output (heart failure). Maladaptive hypertrophy is often a very slow response to easily measured stimuli, which affords for significant intervention potential. Evaluating the metabolic changes associated with maladaptive hypertrophy may allow for treatment methods that seek to correct key metabolites to slow/reverse this disease progression. To elucidate the metabolic changes in response to the effect of EER modification, the investigator submitted heart samples from mice undergoing transverse aortic constriction (TAC) or sham treatment with or without ERR dosing along with heart and quadricep muscle involving additional experimental perturbations. There were three different experimental cohorts within this study. Cohort one consisted of the following heart tissue groups: vehicle sham (n=4), vehicle TAC (n=8), SLU915 sham (n=4), and SLU915 TAC (n=6). Cohort two consisted of muscle tissue derived from mice treated with vehicle (n=7) or the compound SLU-PP-332, while cohort three was comprised of WT (n=5) and klf15 (n=5) mice heart tissue. Heart tissue was normalized based on the mass of sample extracted prior to statistical analysis, while muscle samples were processed in an equivalent manner with no additional normalization prior to statistical analysis. Peak area data were median scaled, and any missing values were imputed with sample set minimums on a per biochemical basis. The provided Excel data tables include the raw data for each sample and the accompanying statistical analysis results are provided in the Heatmap Excel files.

Data provided in the mView product can be quite large and contain a great deal of information. To provide an initial focus for further consideration, a few observations are offered below from a cursory view of the data. These are not presented as a comprehensive analysis; the PI, with a much greater knowledge of the experimental system, is encouraged to make a detailed study of the data for additional or alternative interpretations. For the discussion below, please refer to graphical illustrations in the accompanying PowerPoint file, or to the statistical tables, box plots, and other graphics found in the accompanying client data table. For convenience, biochemicals are highlighted in **bold** text in the report when they correspond to data plots shown in the accompanying figures.

Statistical Overview (Slides 3 and 4): There were a total of 855 and 711 named and unnamed biochemicals detected in the heart and muscle sample datasets respectively. At a significance level of $p < 0.05$ (5% of all detected metabolites), 42 and 36 differences between the groups for heart and muscle samples respectively can be expected from random chance alone. There were greater than these respective numbers in all group comparisons except for the klf15/WT and TAC SLU915/Sham SLU915 heart group comparisons (**Slide 3**). Importantly, these results suggest that the metabolomic profiles

for the heart and muscle samples are significantly impacted by most of the experimental treatments, with the exception of that involving *klf15*.

Principal Component Analysis (Slides 7 and 8): Principal Component Analysis (PCA) (see Appendix, Statistical Methods and Terminology, Section 5) is a mathematical method which can be used to obtain a high-level view of metabolomic datasets. PCA transforms a large number of variables into a smaller number of components, thereby providing a high-level overview of potential similarities and differences within the dataset. Here, within the heart dataset, the vehicle and SLU915 treated groups (Cohort 1) segregated away from the WT and *klf15* groups (Cohort 3) along component 1 of the PCA plot (**Figure 2**, compare light blue, teal, dark blue, pink, orange, and maroon circles). Additionally within cohort 1, the SLU915 sham and SLU915 TAC groups clustered tightly together (suggesting minimal metabolic differences between the groups), while the vehicle TAC exhibited heterogeneity, overlapping to some extent with the vehicle sham, SLU915 sham, and SLU915 TAC groups (**Figure 2**, compare light blue, teal, dark blue, and circles). Little discernable separation was observed however between the *klf15* and WT samples of cohort 3 (**Figure 2**, compare, orange, and maroon circles). Within the muscle dataset, the vehicle and SLU-PP-332 groups segregated loosely throughout components 1 and 2 with some overlap between the groups (**Figure 3**, compare light blue and dark blue circles). Taken together, these PCA results suggest that there are some metabolic differences based on treatment with SLU915 and SLU-PP-332.

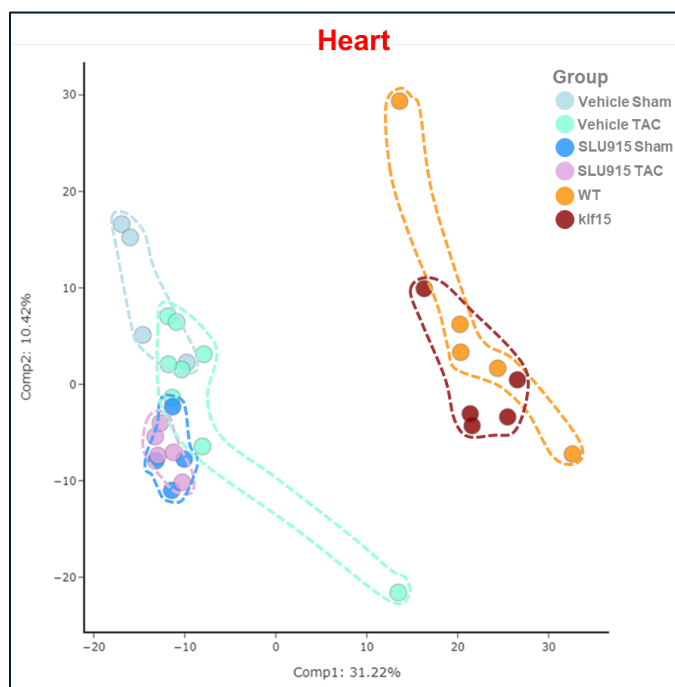


Figure 2. Principal Component Analysis (PCA), showing segregation of heart samples based on group.

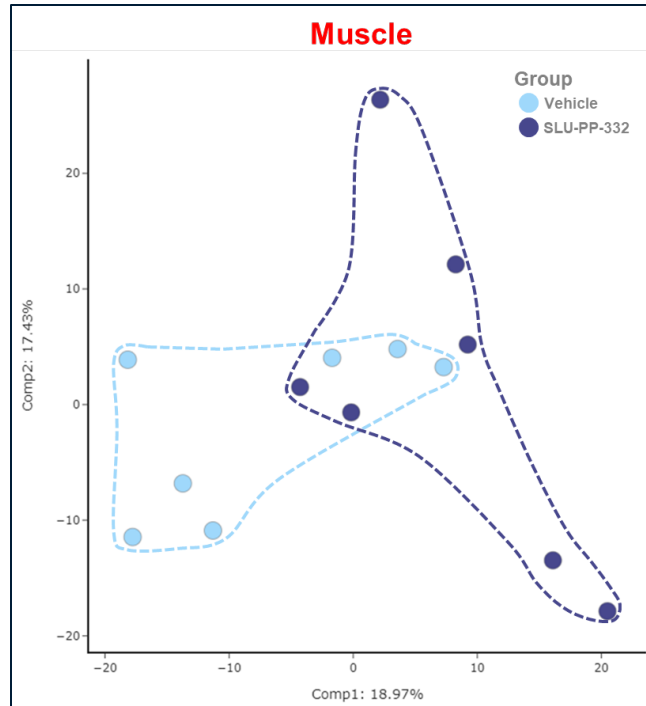


Figure 3. Principal Component Analysis (PCA), showing segregation of muscle samples based on group.

- Differences in carbohydrate and energy metabolites (Slide 9):** Under normal conditions the heart produces ATP for energy via fatty acid oxidation (FAO), with less glucose metabolism for energy, however under stressed conditions FAO is decreased while glucose utilization is increased (PMID: [31185774](#)). These metabolic processes are altered in cardiac hypertrophy and heart disease states (PMID: [31185774](#)). Here with SLU915 treatment under the Sham condition, the heart samples displayed significantly higher levels of glucose and various glycolytic intermediates (e.g., **glucose 6-phosphate** and **dihydroxyacetone phosphate (DHAP)**) and significantly lower levels of TCA related metabolites (e.g., **citrate**, **aconitate [cis or trans]**, and **alpha-ketoglutarate**) (Figure 4). A similar pattern was observed when comparing the TAC vehicle group to the Sham vehicle group. Meanwhile, within the muscle dataset, **glucose** was significantly higher, while **lactate** was trending higher in the SLU-PP-332 group compared to the vehicle group. These differences are suggestive of altered glucose utilization and energy homeostasis in response to ERR treatment and with TAC treatment in the vehicle treated mice.

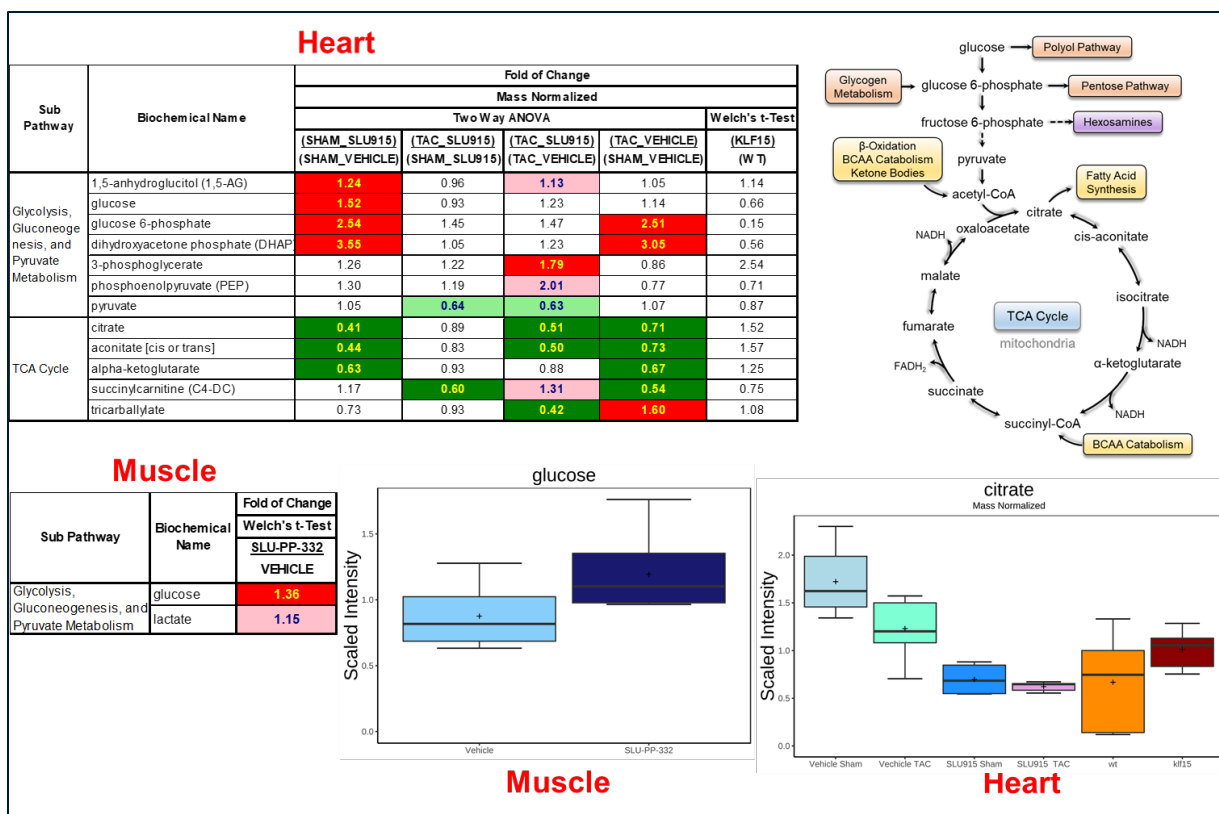


Figure 4. Differences in carbohydrate and energy metabolites in heart and muscle. Red and green shaded cells indicate $p \leq 0.05$ (red indicates the fold change values are significantly higher for that comparison; green values significantly lower). Light red and light green shaded cells indicate $0.05 < p < 0.10$ (light red indicates the fold change values trend higher for that comparison; light green values trend lower).

- Differences in histidine and lysine metabolites (Slide 10):** Methylation of histidine residues is a post-translational modification unique to muscles. Here, the methylated histidine metabolites **1-methylhistidine** and **3-methylhistidine** were significantly higher in the SLU-PP-332 group compared to the vehicle group within the muscle samples, which suggests a higher level of muscle protein breakdown within the SLU-PP-332 group (**Figure 5**). In contrast, within the heart dataset, **3-methylhistidine** was significantly lower in the sham SLU915 and TAC vehicle groups compared to the sham vehicle group (**Figure 5**). Additionally, several other histidine metabolites (e.g., **carnosine** and **anserine**) were significantly altered within the heart dataset group of comparisons, suggesting that SLU915 and TAC treatment altered histidine metabolism within the heart tissue of these mice groups (**Figure 5**). In addition, several lysine metabolites (e.g., **N6-acetyllysine**, **N6**, **N6**, **N6-trimethyllysine**, and **5-hydroxylysine**) were significantly higher in the SLU-PP-332 group when compared to the vehicle group in the muscle dataset (**Figure 4**). Similarly, **5-hydroxylysine** was significantly elevated in the sham SLU915 and TAC vehicle groups compared to the sham vehicle group (**Figure 5**). As with the

changes in the histidine metabolites, these changes could have arisen from increases in protein degradation due to muscle breakdown in response to ERR agonist or TAC treatment (at least within the vehicle treated mice).

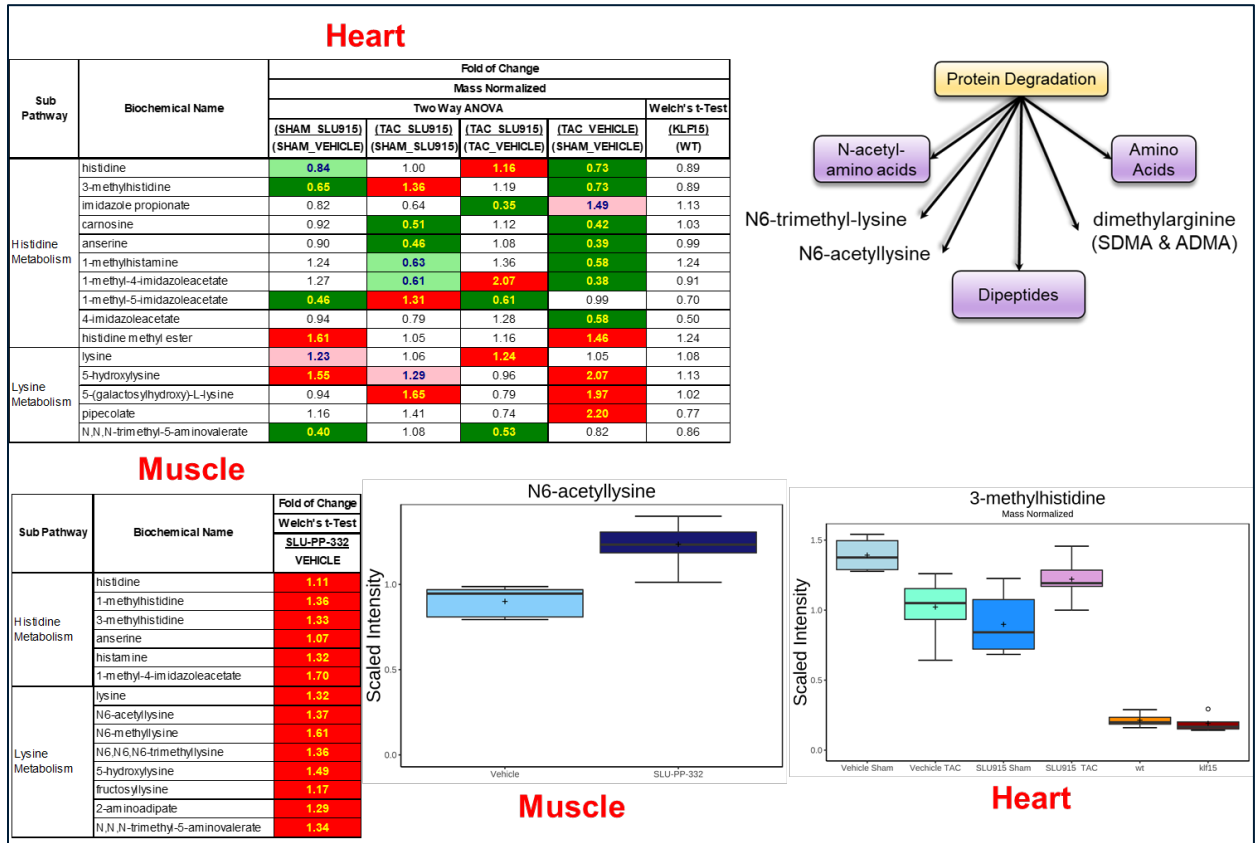


Figure 5. Differences in histidine and lysine related metabolites in heart and muscle. Red and green shaded cells indicate $p \leq 0.05$ (red indicates the fold change values are significantly higher for that comparison; green values significantly lower). Light red and light green shaded cells indicate $0.05 < p < 0.10$ (light red indicates the fold change values trend higher for that comparison; light green values trend lower).

- Differences in arginine and polyamine metabolites (Slide 11):** Arginine contributes to multiple aspects of cellular metabolism, including nitrogen balance (in the urea cycle), inflammatory signaling (in the co-production of nitric oxide and citrulline), and energy metabolism (via the generation of creatine which, as creatine phosphate, serves as a key energy storage compound). In the muscle dataset, **dimethylarginine (SDMA + ADMA)** along with several other arginine metabolites were significantly higher in the SLU-PP-332 group compared to the vehicle group (**Figure 6**). There is evidence that **dimethylarginine (SDMA + ADMA)** is elevated in the plasma of cardiac patients with hypertrophic cardiomyopathy (PMID: [31337005](https://pubmed.ncbi.nlm.nih.gov/31337005/)). Arginine supplementation enhances collagen deposition and improves wound strength in humans and rodents (PMID: [16207646](https://pubmed.ncbi.nlm.nih.gov/16207646/)). Collagen is

a major component of the extracellular matrix (ECM) that gives tissues a rigid structure and provides a configuration for attachment. Proline accounts for one third of the amino acid composition of collagen. Higher levels of **pro-hydroxy-pro** in heart, as observed here in the SLU915 and TAC treated groups, could be interpreted as the result of ECM remodeling in response to ERR. TAC treatment led to increases in **trans-4-hydroxyproline** as well, though statistical significance was observed only in the TAC treated vehicle group (**Figure 6**). TAC treatment within the SLU915 treated mice did however lead to significant elevations in several polyamine metabolites (e.g., **putrescine**, **N-acetylputrescine**, and **spermidine**), though this response was also observed with TAC in the vehicle treated mice (**Figure 6**). Altered levels of arginine could be indicative of altered nitric oxide production which is supported by the observed higher levels of polyamine metabolites. These changes could also be supportive of tissue damage in response to ERR or TAC treatment.

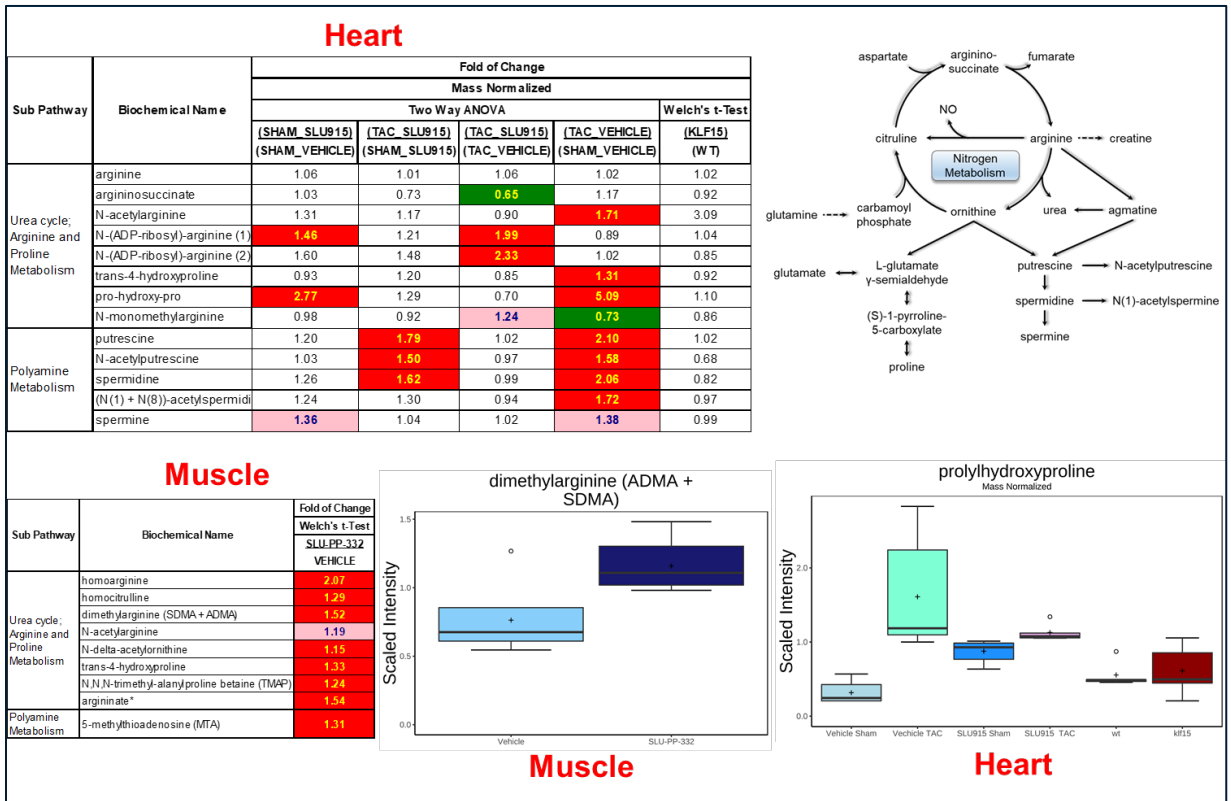


Figure 6. Differences in arginine and polyamine metabolites in heart and muscle. Red and green shaded cells indicate $p \leq 0.05$ (red indicates the fold change values are significantly higher for that comparison; green values significantly lower). Light red and light green shaded cells indicate $0.05 < p < 0.10$ (light red indicates the fold change values trend higher for that comparison; light green values trend lower).

- **Differences in lipid and fatty acid metabolism (Slides 12 and 13):** Phosphatidylcholine and phosphatidylethanolamine make up the largest proportion of membrane phospholipids. Phospholipids include glycerophospholipids, plasmalogens, and sphingomyelins. Phospholipids are prevalent in lipid membranes and are necessary for cell growth and survival. Several phospholipid related metabolites such as **1-palmitoyl-2-stearoyl-GPC (16:0/18:0)**, **1-stearoyl-2-oleoyl-GPC (18:0/18:1)**, and **1-palmitoyl-2-stearoyl-GPE (16:0/18:0)*** were significantly lower in the sham SLU915 and TAC vehicle heart groups compared to the sham vehicle group (**Figure 7**). In contrast within the muscle group comparisons, phospholipid metabolites (e.g., **glycerophosphorylcholine (GPC)** and **1-palmitoyl-2-stearoyl-GPC (16:0/18:0)**) were significantly higher in the SLU-PP-332 group. The different levels of these metabolites could correlate with altered lipid synthesis or cell proliferation.

Long-chain fatty acids (LCFA) destined for oxidation are conjugated to carnitine by the outer mitochondrial membrane carnitine-palmitoyltransferase 1 which results in the release of CoA. The acylcarnitines are then transported across the intermembrane space by carnitine/acylcarnitine translocase and acted upon by the inner membrane carnitine-palmitoyl transferase 2 which releases carnitine and reconjugates the LCFA with CoA for mitochondrial fatty acid beta-oxidation. As mentioned in the previous section, under normal conditions, the majority of cardiac ATP is provided through fatty acid oxidation. Under stress conditions, fatty acid oxidation may be reduced with an associated increase in glucose metabolism. Here within the heart samples, medium chain fatty acids, LCFAs (e.g., **caprate (10:0)** and **hexadecatrienoate (16:3n3)**), as well as several carnitine-conjugated fatty acids (e.g., **octanoylcarnitine (C8)**, **laurylcarnitine (C12)**, and **palmitoleoylcarnitine (C16:1)***) were found to be significantly lower within the sham SLU915 and TAC vehicle groups when each was compared to the Sham vehicle group (**Figure 8**). Interestingly, within the muscle group, the fatty acid metabolite **2-hydroxyadipate** and carnitine metabolite **deoxycarnitine** were significantly higher in the SLU-PP-332 group compared to the vehicle group (**Figure 8**). These data are suggestive of significant alterations in lipid and fatty acid metabolism in the ERR and TAC treatments compared to the respective controls.

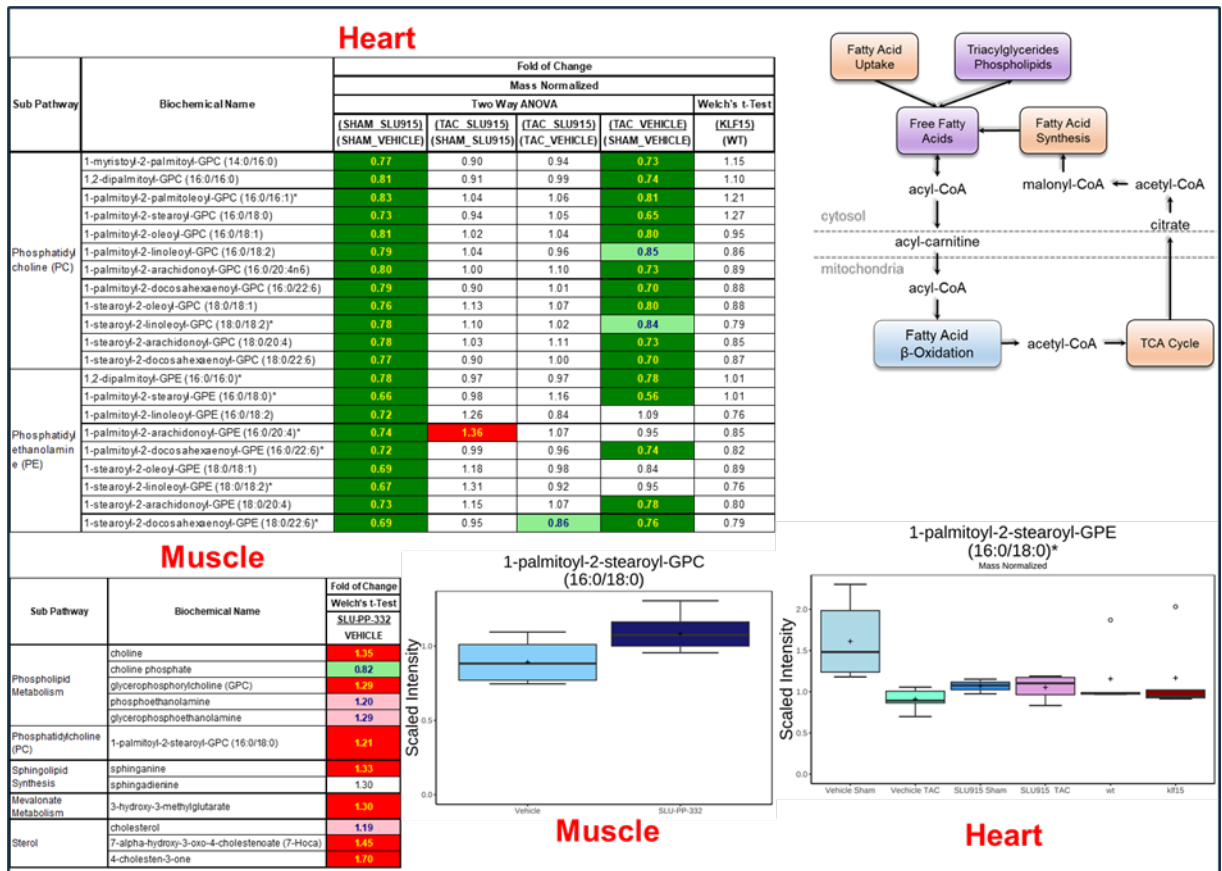


Figure 7. Differences in lipid metabolism in heart and muscle. Red and green shaded cells indicate $p \leq 0.05$ (red indicates the fold change values are significantly higher for that comparison; green values significantly lower). Light red and light green shaded cells indicate $0.05 < p < 0.10$ (light red indicates the fold change values trend higher for that comparison; light green values trend lower).

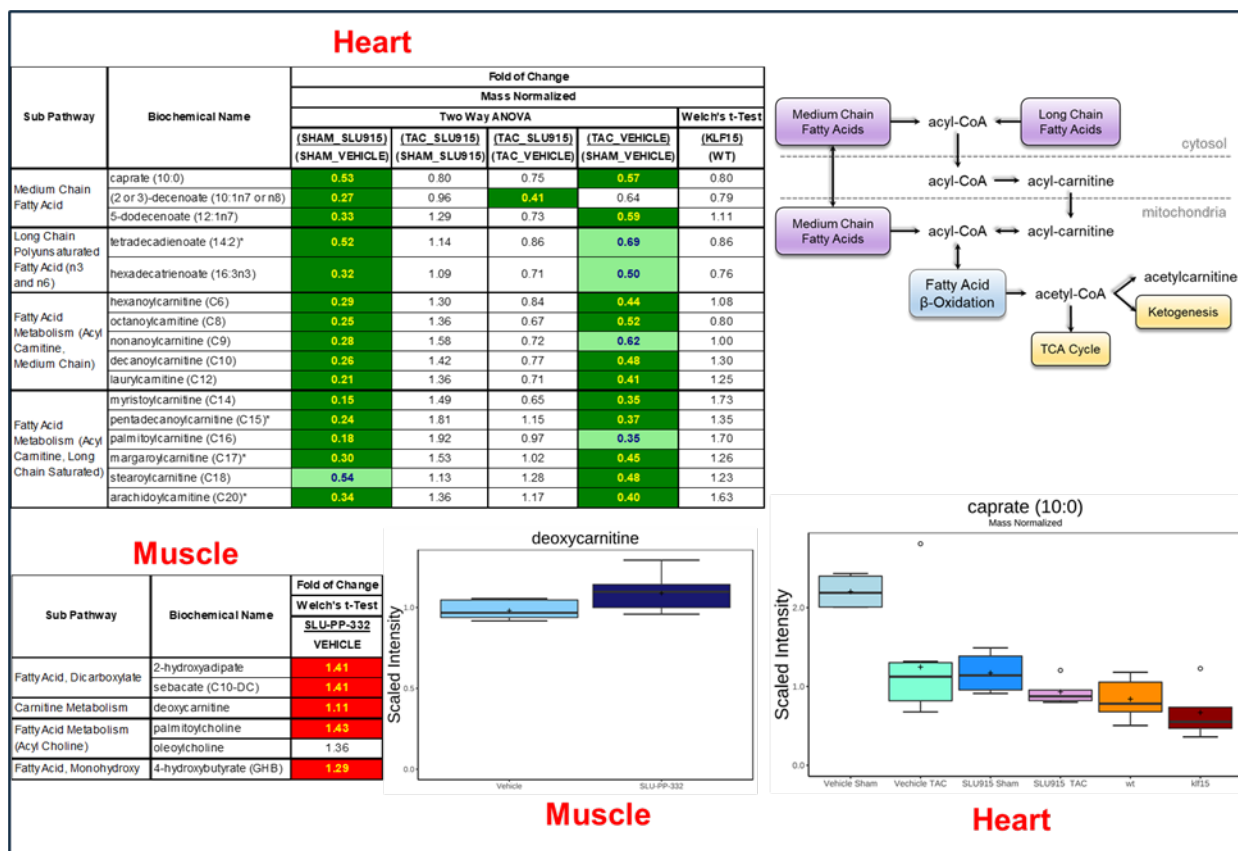


Figure 8. Differences in fatty acid metabolism in heart and muscle. Red and green shaded cells indicate $p \leq 0.05$ (red indicates the fold change values are significantly higher for that comparison; green values significantly lower). Light red and light green shaded cells indicate $0.05 < p < 0.10$ (light red indicates the fold change values trend higher for that comparison; light green values trend lower).

- Differences in oxidative stress metabolites (Slide 14):** Oxidative stress can occur when there is an imbalance between free radical or reactive oxygen species (ROS) and antioxidant defenses. The free radicals can then cause lipid peroxidation and protein and DNA/RNA oxidation. The glutathione system plays important roles in antioxidant defense, redox-homeostasis, and detoxification of xenobiotics. ROS have been shown to be elevated in a TAC model that induced cardiac pressure overload, which was reversed via treatment with an ROS scavenger (PMID: [24951621](#)). Several glutathione pathway metabolites (e.g., **gamma-glutamylthreonine** and **gamma-glutamylvaline**) were significantly altered within the heart samples of the sham SLU915 or TAC vehicle groups compared to the sham vehicle group (**Figure 9**). In the SLU-PP-332 muscle group, glutathione pathway metabolites (e.g., **S-adenosylmethionine (SAM)** and **gamma-glutamylvaline**) were significantly higher compared to the vehicle group (**Figure 9**). These data suggest an altered state of oxidative stress within the ERR and TAC treated mice possibly associated with changes in lipid and fatty acid metabolism, glycolysis, and TCA energy homeostasis.

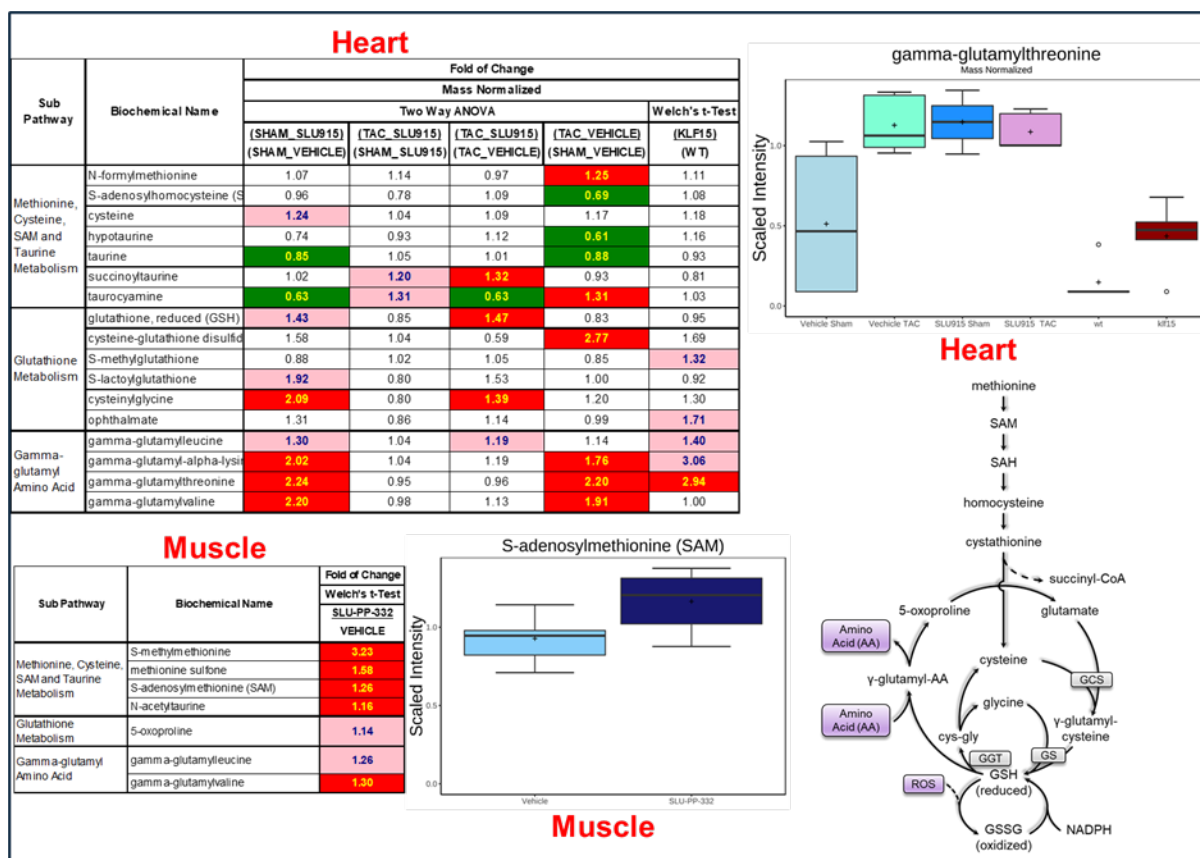


Figure 9. Differences in oxidative stress metabolites in heart and muscle. Red and green shaded cells indicate $p \leq 0.05$ (red indicates the fold change values are significantly higher for that comparison; green values significantly lower). Light red and light green shaded cells indicate $0.05 < p < 0.10$ (light red indicates the fold change values trend higher for that comparison; light green values trend lower).

- Additional observation of potential interest:** It is worth mentioning that within the heart dataset, the chemical metabolite **ethylparaben sulfate** was significantly higher in both the Sham SLU915 and TAC SLU915 groups compared to the sham vehicle control groups (See heatmap dataset). Parabens including **ethylparaben** have been shown display estrogen like activity increasing estrogen-responsive biomarkers and interacting with the estrogen binding pocket of the human estrogen receptor alpha (PMID: [27121550](https://pubmed.ncbi.nlm.nih.gov/27121550/)), which may warrant further investigation.

Conclusions

These data sets of mouse heart and muscle samples gave a robust set of metabolites for analysis and the comparisons between the TAC, SLU915, and SLU-PP-332 and respective control mice resulted in some interesting findings. Most notably, there were indications of differences in carbohydrate and energy metabolites, histidine and lysine metabolism, arginine and polyamine metabolism, lipid and fatty acid metabolism, oxidative stress metabolites, and the chemical metabolite ethylparaben sulfate. Interestingly, the discussed metabolic effects of SLU915 within the heart appear to be frequently contrasting with the effects of SLU-PP-332 in the muscle tissue, which could be a tissue specific effect of ERR treatment or may represent differences in SLU915 and SLU-PP-332 mechanisms of action.

Possible paths forward:

- Global metabolomic profiling of heart, muscle, and serum samples from mice treated with SLU915 or SLU-PP-332 to see if metabolic changes are tissue or ERR drug specific.

Study Parameters

Data Quality: Instrument and Process Variability

QC Sample	Measurement	Median RSD Quadricep
Internal Standards	Instrument Variability	5%
Endogenous Biochemicals	Total Process Variability	8%

QC Sample	Measurement	Median RSD Heart
Internal Standards	Instrument Variability	4%
Endogenous Biochemicals	Total Process Variability	9%

Instrument variability was determined by calculating the median relative standard deviation (RSD) for the internal standards that were added to each sample prior to injection into the mass spectrometers. Overall process variability was determined by calculating the median RSD for all endogenous metabolites (i.e., non-instrument standards) present in 100% of the Client Matrix samples, which are technical replicates of pooled client samples. Values for instrument and process variability meet Metabolon's acceptance criteria as shown in the table above.

Appendix

Metabolon Platform

Sample Accessioning: Following receipt, samples were inventoried and immediately stored at -80°C. Each sample received was accessioned into the Metabolon LIMS system and was assigned by the LIMS a unique identifier that was associated with the original source identifier only. This identifier was used to track all sample handling, tasks, results, etc. The samples (and all derived aliquots) were tracked by the LIMS system. All portions of any sample were automatically assigned their own unique identifiers by the LIMS when a new task was created; the relationship of these samples was also tracked. All samples were maintained at -80°C until processed.

Sample Preparation: Samples were prepared using the automated MicroLab STAR® system from Hamilton Company. Several recovery standards were added prior to the first step in the extraction process for QC purposes. To remove protein, dissociate small molecules bound to protein or trapped in the precipitated protein matrix, and to recover chemically diverse metabolites, proteins were precipitated with methanol under vigorous shaking for 2 min (Glen Mills GenoGrinder 2000) followed by centrifugation. The resulting extract was divided into five fractions: two for analysis by two separate reverse phase (RP)/UPLC-MS/MS methods with positive ion mode electrospray ionization (ESI), one for analysis by RP/UPLC-MS/MS with negative ion mode ESI, one for analysis by HILIC/UPLC-MS/MS with negative ion mode ESI, and one sample was reserved for backup. Samples were placed briefly on a TurboVap® (Zymark) to remove the organic solvent. The sample extracts were stored overnight under nitrogen before preparation for analysis.

QA/QC: Several types of controls were analyzed in concert with the experimental samples: a pooled matrix sample generated by taking a small volume of each experimental sample (or alternatively, use of a pool of well-characterized human plasma) served as a technical replicate throughout the data set; extracted water samples served as process blanks; and a cocktail of QC standards that were carefully chosen not to interfere with the measurement of endogenous compounds were spiked into every analyzed sample, allowed instrument performance monitoring and aided chromatographic alignment. Tables 1 and 2 describe these QC samples and standards. Instrument variability was determined by calculating the median relative standard deviation (RSD) for the standards that were added to each sample prior to injection into the mass spectrometers. Overall process variability was determined by calculating the median RSD for all endogenous metabolites (i.e., non-instrument standards) present in 100% of the pooled matrix samples. Experimental samples were randomized across the platform run with QC samples spaced evenly among the injections, as outlined in Figure 1.

Table 1: Description of Metabolon QC Samples

Type	Description	Purpose
MTRX	Large pool of human plasma maintained by Metabolon that has been characterized extensively.	Assure that all aspects of the Metabolon process are operating within specifications.
CMTRX	Pool created by taking a small aliquot from every customer sample.	Assess the effect of a non-plasma matrix on the Metabolon process and distinguish biological variability from process variability.
PRCS	Aliquot of ultra-pure water	Process Blank used to assess the contribution to compound signals from the process.
SOLV	Aliquot of solvents used in extraction.	Solvent Blank used to segregate contamination sources in the extraction.

Table 2: Metabolon QC Standards

Type	Description	Purpose
RS	Recovery Standard	Assess variability and verify performance of extraction and instrumentation.
IS	Internal Standard	Assess variability and performance of instrument.

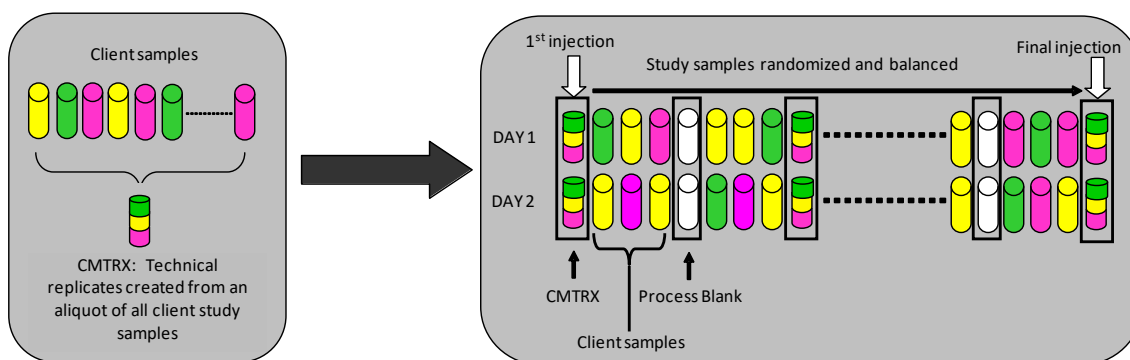


Figure 1. Preparation of client-specific technical replicates. A small aliquot of each client sample (colored cylinders) is pooled to create a CMTRX technical replicate sample (multi-colored cylinder), which is then injected periodically throughout the platform run. Variability among consistently detected biochemicals can be used to calculate an estimate of overall process and platform variability.

Ultrahigh Performance Liquid Chromatography-Tandem Mass Spectroscopy (UPLC-MS/MS): All methods utilized a Waters ACQUITY ultra-performance liquid chromatography (UPLC) and a Thermo Scientific Q-Exactive high resolution/accurate mass spectrometer interfaced with a heated electrospray ionization (HESI-II) source and Orbitrap mass analyzer operated at 35,000 mass resolution. The sample extract was dried then reconstituted in solvents compatible to each of the four methods. Each reconstitution solvent contained a series of standards at fixed concentrations to ensure injection and chromatographic consistency. One aliquot was analyzed using acidic positive ion conditions, chromatographically optimized for more hydrophilic compounds. In this method, the extract was gradient eluted from a C18 column (Waters UPLC BEH C18-2.1x100 mm, 1.7 μ m) using water and methanol, containing 0.05% perfluoropentanoic acid (PFPA) and 0.1% formic acid (FA). Another aliquot was also analyzed using acidic positive ion conditions, however it was chromatographically optimized for more hydrophobic compounds. In this method, the extract was gradient eluted from the same afore mentioned C18 column using methanol, acetonitrile, water, 0.05% PFPA and 0.01% FA and was operated at an overall higher organic content. Another aliquot was analyzed using basic negative ion optimized conditions using a separate dedicated C18 column. The basic extracts were gradient eluted from the column using methanol and water, however with 6.5mM Ammonium Bicarbonate at pH 8. The fourth aliquot was analyzed via negative ionization following elution from a HILIC column (Waters UPLC BEH Amide 2.1x150 mm, 1.7 μ m) using a gradient consisting of water and acetonitrile with 10mM Ammonium Formate, pH 10.8. The MS analysis alternated between MS and data-dependent MSⁿ scans using dynamic exclusion. The scan range varied slightly between methods but covered 70-1000 m/z. Raw data files are archived and extracted as described below.

Bioinformatics: The informatics system consisted of four major components, the Laboratory Information Management System (LIMS), the data extraction and peak-identification software, data processing tools for QC and compound identification, and a collection of information interpretation and visualization tools for use by data analysts. The hardware and software foundations for these informatics components were the LAN backbone, and a database server running Oracle 10.2.0.1 Enterprise Edition.

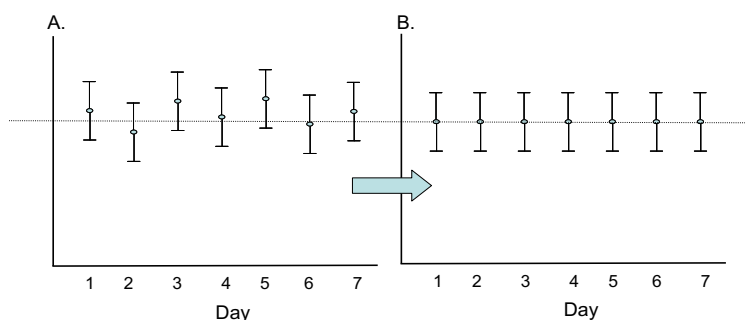
LIMS: The purpose of the Metabolon LIMS system was to enable fully auditable laboratory automation through a secure, easy to use, and highly specialized system. The scope of the Metabolon LIMS system encompasses sample accessioning, sample preparation and instrumental analysis and reporting and advanced data analysis. All of the subsequent software systems are grounded in the LIMS data structures. It has been modified to leverage and interface with the in-house information extraction and data visualization systems, as well as third party instrumentation and data analysis software.

Data Extraction and Compound Identification: Raw data was extracted, peak-identified and QC processed using Metabolon's hardware and software. These systems are built on a web-service platform utilizing Microsoft's .NET technologies, which run on high-performance application servers and fiber-channel storage arrays in clusters to provide active failover and load-balancing. Compounds were identified by comparison to library entries of purified standards or recurrent unknown entities. Metabolon maintains

a library based on authenticated standards that contains the retention time/index (RI), mass to charge ratio (m/z), and chromatographic data (including MS/MS spectral data) on all molecules present in the library. Furthermore, biochemical identifications are based on three criteria: retention index within a narrow RI window of the proposed identification, accurate mass match to the library ± 10 ppm, and the MS/MS forward and reverse scores between the experimental data and authentic standards. The MS/MS scores are based on a comparison of the ions present in the experimental spectrum to the ions present in the library spectrum. While there may be similarities between these molecules based on one of these factors, the use of all three data points can be utilized to distinguish and differentiate biochemicals. More than 3300 commercially available purified standard compounds have been acquired and registered into LIMS for analysis on all platforms for determination of their analytical characteristics. Additional mass spectral entries have been created for structurally unnamed biochemicals, which have been identified by virtue of their recurrent nature (both chromatographic and mass spectral). These compounds have the potential to be identified by future acquisition of a matching purified standard or by classical structural analysis.

Curation: A variety of curation procedures were carried out to ensure that a high quality data set was made available for statistical analysis and data interpretation. The QC and curation processes were designed to ensure accurate and consistent identification of true chemical entities, and to remove those representing system artifacts, mis-assignments, and background noise. Metabolon data analysts use proprietary visualization and interpretation software to confirm the consistency of peak identification among the various samples. Library matches for each compound were checked for each sample and corrected if necessary.

Metabolite Quantification and Data Normalization: Peaks were quantified using area-under-the-curve. For studies spanning multiple days, a data normalization step was performed to correct variation resulting from instrument inter-day tuning differences. Essentially, each compound was corrected in run-day blocks by registering the medians to equal one (1.00) and normalizing each data point proportionately (termed the “block correction”; Figure 2). For studies that did not require more than one day of analysis, no normalization is necessary, other than for purposes of data visualization. In certain instances, biochemical data may have been normalized to an additional factor (e.g., cell counts, total protein as determined by Bradford assay, osmolality, etc.) to account for differences in metabolite levels due to differences in the amount of material present in



each sample.

Figure 2: Visualization of data normalization steps for a multiday platform run.

Statistical Methods and Terminology

Statistical Calculations: For many studies, two types of statistical analysis are usually performed: (1) significance tests and (2) classification analysis. Standard statistical analyses are performed in ArrayStudio on log transformed data. For those analyses not standard in ArrayStudio, the programs R (<http://cran.r-project.org/>) or JMP are used. Below are examples of frequently employed significance tests and classification methods followed by a discussion of p- and q-value significance thresholds.

1. Welch's two-sample *t*-test

Welch's two-sample *t*-test is used to test whether two unknown means are different from two independent populations.

This version of the two-sample *t*-test allows for unequal variances (variance is the square of the standard deviation) and has an *approximate t*-distribution with degrees of freedom estimated using Satterthwaite's approximation. The test statistic is given by $t = (\bar{x}_1 - \bar{x}_2) / \sqrt{s_1^2/n_1 + s_2^2/n_2}$, and the degrees of freedom is

given by $\left(\frac{s_1^2}{n_1} + \frac{s_2^2}{n_2} \right)^2 / \left(\frac{\left(\frac{s_1^2}{n_1} \right)^2}{n_1 - 1} + \frac{\left(\frac{s_2^2}{n_2} \right)^2}{n_2 - 1} \right)$, where \bar{x}_1, \bar{x}_2 are the sample means, s_1, s_2 ,

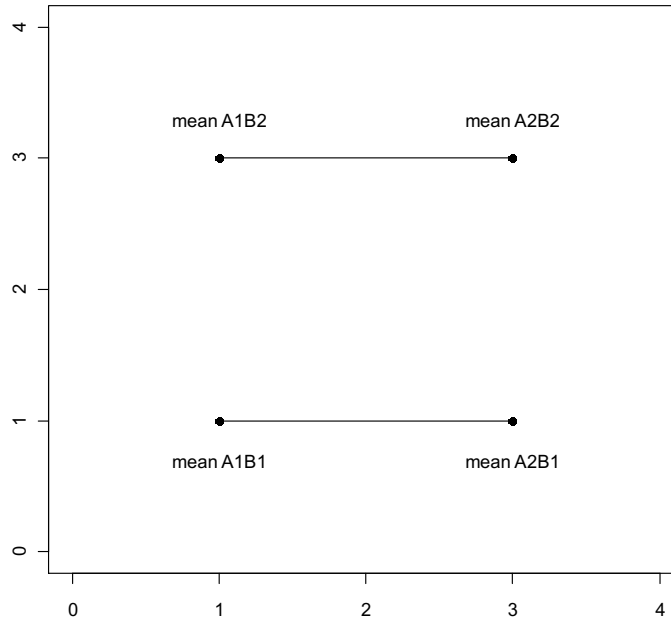
are the sample standard deviations, and n_1, n_2 are the samples sizes from groups 1 and 2, respectively. We typically use a two-sided test (tests whether the means are different) as opposed to a one-sided test (tests whether one mean is greater than the other).

2. Two-way ANOVA

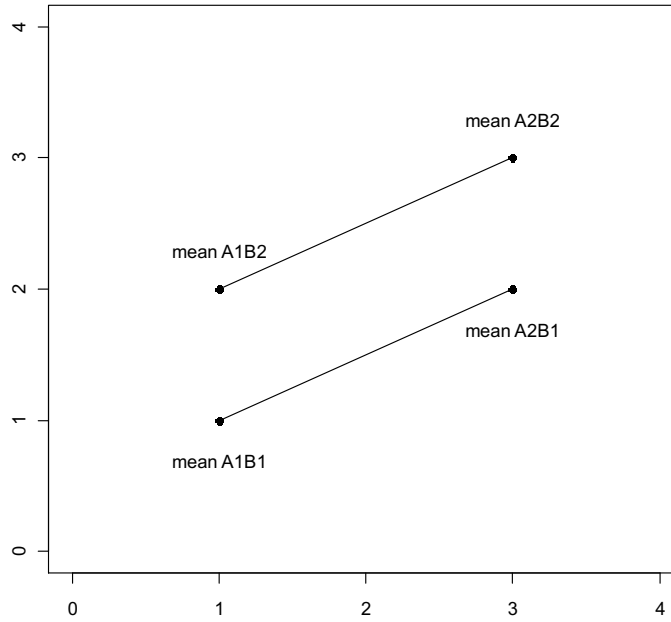
ANOVA stands for analysis of variance. For ANOVA, it is assumed that all populations have the same variances. For a two-way ANOVA, three statistical tests are typically performed: the main effect of each factor and the interaction. Suppose we have two factors A and B, where A represent the genotype and B represent the diet in a mouse study. Suppose each of these factors has two levels (A: wild type, knock out; B: standard diet, high fat diet). For this example, there are 4 combinations ("treatments"): A1B1, A1B2, A2B1, A2B2. The overall ANOVA F-test gives the p-value for testing whether all four of these means are equal or whether at least one pair is different. However, we are also interested in the effect of the genotype and diet. A main effect is a contrast that tests one factor across the levels of the other factor. Hence the A main effect compares (A1B1 + A1B2)/2 vs. (A2B1 + A2B2)/2, and the B-main effect compares (A1B1 + A2B1)/2 vs. (A1B2 + A2B2)/2. The interaction is a contrast that tests whether the mean difference for one factor depends on the level of the other factor, which is (A1B2 + A2B1)/2 vs. (A1B1 + A2B2)/2.

Some sample plots follow. For the first plot, there is a B main effect, but no A main effect and no interaction, as the effect of B does not depend on the level of A. For the second plot, notice how the mean difference for B is the same at each level of A and the difference in A is the same for each level of B, hence there is no statistical interaction. The final plot also has main effects for A and B, but here also has an interaction: we see the effect of B depends on the level of A (0 for A1 but 2 for A2), i.e., the effect of the diet depends on the genotype. We also see here the interpretation of the main effects depends on whether there is an interaction or not.

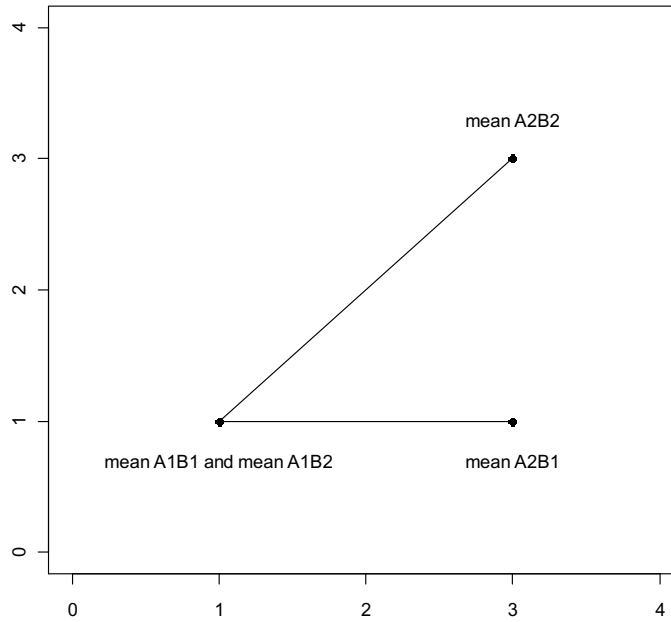
Main Effect for B, but no Main Effect for A, no Interaction



Main Effect for A, Main Effect for B, No Interaction



Main Effect for A, Main Effect for B, with Interaction



3. p- values

For statistical significance testing, p-values are given. The lower the p-value, the more evidence we have that the null hypothesis (typically that two population means are equal) is not true. If “statistical significance” is declared for p-values less than 0.05, then 5% of the time we incorrectly conclude the means are different, when actually they are the same.

The p-value is the probability that the test statistic is at least as extreme as observed in this experiment given that the null hypothesis is true. Hence, the more extreme the statistic, the lower the p-value and the more evidence the data gives against the null hypothesis.

4. q-values

The level of 0.05 is the false positive rate when there is one test. However, for a large number of tests we need to account for false positives. There are different methods to correct for multiple testing. The oldest methods are family-wise error rate adjustments (Bonferroni, Tukey, etc.), but these tend to be extremely conservative for a very large number of tests. With gene arrays, using the False Discovery Rate (FDR) is more common. The family-wise error rate adjustments give one a high degree of confidence that there are zero false discoveries. However, with FDR methods, one can allow for a small number of false discoveries. The FDR for a given set of compounds can be estimated using the q-value (see Storey J and Tibshirani R. (2003) Statistical significance for genomewide studies. Proc. Natl. Acad. Sci. USA 100: 9440-9445; PMID: 12883005).

In order to interpret the q-value, the data must first be sorted by the p-value then choose the cutoff for significance (typically $p < 0.05$). The q-value gives the false discovery rate for the selected list (i.e., an estimate of the proportion of false discoveries for the list of compounds whose p-value is below the cutoff for significance). For Table 1 below, if the whole list is declared significant, then the false discovery rate is approximately 10%. If everything from Compound 079 and above is declared significant, then the false discovery rate is approximately 2.5%.
Table 1: Example of q-value interpretation

Compound	p-value	q-value
Compound 103	0.0002	0.0122
Compound 212	0.0004	0.0122
Compound 076	0.0004	0.0122
Compound 002	0.0005	0.0122
Compound 168	0.0006	0.0122
Compound 079	0.0016	0.0258
Compound 113	0.0052	0.0631
Compound 050	0.0053	0.0631
Compound 098	0.0061	0.0647
Compound 267	0.0098	0.0939

5. Principal Components Analysis (PCA)

Principal components analysis is an unsupervised analysis that reduces the dimension of the data. Each principal component is a linear combination of every metabolite and the principal components are uncorrelated. The number of principal components is equal to the number of observations.

The first principal component is computed by determining the coefficients of the metabolites that maximizes the variance of the linear combination. The second component finds the coefficients that maximize the variance with the condition that the second component is orthogonal to the first. The third component is orthogonal to the first two components and so on. The total variance is defined as the sum of the variances of the predicted values of each component (the variance is the square of the standard deviation), and for each component, the proportion of the total variance is computed. For example, if the standard deviation of the predicted values of the first principal component is 0.4 and the total variance = 1, then $100 \times 0.4 \times 0.4 / 1 = 16\%$ of the total variance is explained by the first component. Since this is an unsupervised method, the main components may be unrelated to the treatment groups, and the “separation” does not give an estimate of the true predictive ability.